

DPP Dyes as Ligands in Transition-Metal Complexes

Ingo-Peter Lorenz,^{*,[a]} Michael Limmert,^[b] Peter Mayer,^[a] Holger Piotrowski,^[a] Heinz Langhals,^[c] Martin Poppe,^[c] and Kurt Polborn^[c]

Dedicated to Professor Wolfgang Beck on the occasion of his 70th birthday

Abstract: The DPP dyes (=diketopyrrolopyrrole) **1** are deprotonated to give the corresponding dianions **2**. These are treated with two moles of the transition-metal complexes $[L_nMX] = [(Ph_3P)_2MX]$ ($M = Cu, Ag; X = Cl, NO_3$), $[(Ph_3P)AuCl]$, $[(Et_3P)AuCl]$, $[(tBuNC)AuCl]$, $[(Ph_3P)_2PdCl_2]$, and $[(Ph_3P)_2PtCl_2]$ to give the novel bismetalated DPP dyes $[L_nM-N(C_3R^1(O))_2-N-ML_n]$ (**4–10**). In comparison with the starting materials, these compounds show better solubilities, high fluorescence quantum yields ($\Phi \geq 80\%$), and bathochromic absorptions. The com-

pounds **4c**, **5a**, **6b**, **6c**, **6e**, **7c**, and **8c** were characterized by X-ray crystallography. The copper and silver atoms in **4c** and **5a** are trigonal planar and are surrounded by the P atoms of the phosphane ligands and the N atom of the DPP dianion **2**. Both metals are somewhat forced out-of-plane, and the P_2M plane and the phenyl planes of R^1 are twisted by $>70^\circ$ and $<25^\circ$, respec-

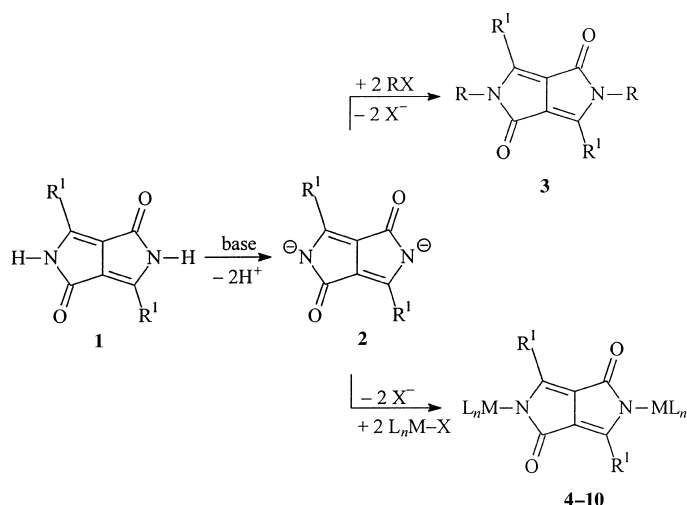
Keywords: coinage metal complexes • dyes • fluorescence • structure elucidation • UV/Vis spectroscopy

tively, towards the chromophore plane. The gold atoms in **6–8** are linearly coordinated to one N and one P (**6b**, **c**, **7c**) or one C atom (**8c**), respectively. The gold atoms are only slightly pressed out-of-plane, and the P substituents are staggered so that there is enough space for the planarization of R^1 into the plane of the chromophore. Compound **8c** shows intermolecular $d^{10}-d^{10}$ interactions between Au^I centers of different molecules, and these interactions lead to infinite chains of parallel orientated molecules in a *gauche* conformation of neighbors (torsion angle = 150°) in the crystal.

Introduction

We recently reported the substitution reaction of some transition-metal complexes with DPP dye derivatives to obtain the first DPP complexes, which exhibit interesting new properties (DPP = diketopyrrolopyrrole).^[1] The diaryl DPP dyes **1** are one of the most recently developed classes of technical pigments,^[2] the remarkable properties of which, such as high light fastness, extraordinary thermal stability, and very low solubility, are supported by the formation of intermolecular $N \cdots H \cdots O$ hydrogen bonds. Unfortunately, such hydrogen bonds diminish fluorescence quantum yields in many cases, hence the use of **1** for fluorescence applications is limited. The fluorescence quantum yield of the phenyl

derivative ($R^1 = C_6H_5$) **1a**, for instance, was found to be only 50%.^[3] The formation of hydrogen bonds can be inhibited by alkylation^[4] or arylation^[5] of the nitrogen atoms (derivatives of the type **3**, Scheme 1). This blocking results in an increase of the fluorescence quantum yields by several percent and in a



Scheme 1. Actual and expected derivatives of DPP dyes.

[a] Prof. Dr. I.-P. Lorenz, Dr. P. Mayer, Dr. H. Piotrowski
Department Chemie, Universität München
Butenandtstrasse 5-3 (Haus D), 81377 München (Germany)
Fax: (+49) 89/2810-7867
E-mail: ipl@cup.uni-muenchen.de

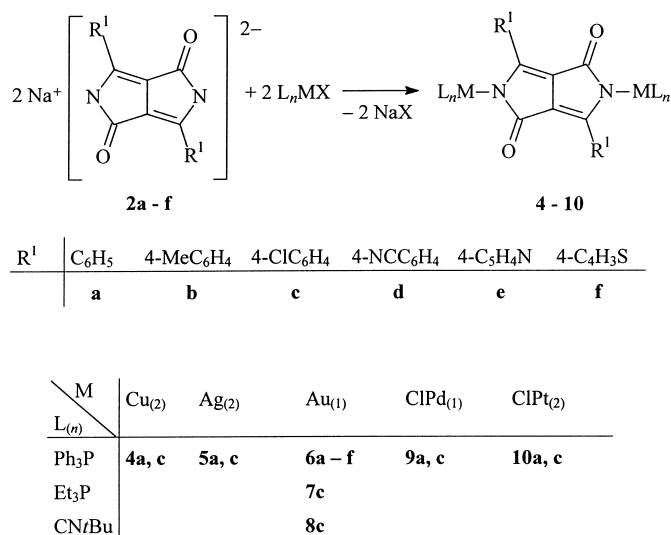
[b] Dr. M. Limmert
University of Exeter, School of Chemistry
Stocker Road, Exeter EX44QD (UK)

[c] Prof. Dr. H. Langhals, Dr. M. Poppe, Dr. K. Polborn
Department Chemie, Universität München
Butenandtstrasse 5-13 (Haus F), 81377 München (Germany)

hypsochromic shift of the absorption maximum in the UV/Vis spectra. A further possibility for the blocking of these positions is the coordination of the nitrogen atoms to metal ions to give complexes of the type **4–10** (Scheme 1).^[1] In a preliminary communication we used complex fragments of Group 11 metals. Bulky substituents like phosphanes on at least one further coordination site prevented the formation of polymeric networks and shielded the entire chromophore against external influence. The result was novel DPP dye complexes with excellent fluorescence properties.^[1] A very high quantum yield in one case indicated the unprecedented effect of efficient support of fluorescence by bulky gold substituents. This was attributed to the complete planarization of the chromophore, including the phenyl substituents R^1 .^[6] Herein, the reactions of DPP dianions with complexes of the type $[(Ph_3P)_2MX]$ ($M = Cu, Ag; X = Cl, NO_3$), $[LAuX]$ ($L = PPh_3, PEt_3, CNtBu; X = Cl$), $[(Ph_3P)_2PdCl_2]$, and $[(Ph_3P)_2PtCl_2]$ will be reported in detail (Scheme 1).

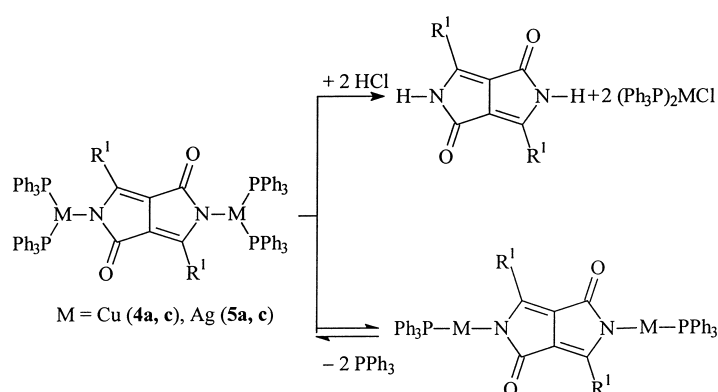
Results and Discussion

Synthetic aspects: Analogously to the N-alkylation,^[4] the red DPP pigment **1a–f** was treated first with two equivalents of hexamethyldisilazane sodium ($=NaN(Si(CH_3)_3)_2$) in DMF to give the deep blue dianion of DPP (**2a–f**). Subsequently it was added to a suitable transition-metal salt or complex, for example, $[(Ph_3P)_2MX]$ ($M = Cu, Ag; X = Cl, NO_3$), $[LAuX]$ ($L = PPh_3, PEt_3, CNtBu; X = Cl$), or $[(Ph_3P)_2MCl_2]$ ($M = Pd, Pt$). The products **4–10** precipitated, either directly from the reaction mixture or after recrystallizing the crude product, as intensely colored, brilliant red to purple solids in good yield (Scheme 2). They are soluble in chlorinated hydrocarbons,



Scheme 2. Synthesis of the transition-metal complexes of dyes **4–10**.

but **5a,c** and, to a smaller extent, **4a,c** and **9a,c** slowly decompose in CHCl₃. This is due to traces of HCl therein, which reprotonate the lactam-N (Scheme 3). The lightfastness of the dissolved complexes is limited to a few weeks, whereby **6c** lasted by far the longest period. In our experience, this is



Scheme 3. Elimination processes of the dye complexes **4a,c** and **5a,c**.

comparable to the N-alkylated derivatives. In the solid state, especially the gold complexes (except **7c**), can be stored for months under argon in the dark at RT, and even for weeks under air without detectable decomposition products.

Generally, well-defined products are obtained only when using “soft” nonoxophilic metal ions like Ag⁺, Au⁺, and Pt²⁺ (e.g. in $[(Ph_3P)_2MX]$ ($M = Cu, Ag; X = Cl, NO_3$), $[LAuX]$ ($L = PPh_3, PEt_3, CNtBu; X = Cl$), and $[(Ph_3P)_2PtCl_2]$) along with bulky ligands like $L = PPh_3$. These stabilize the products by preventing intermolecular interactions as a result of their steric demand. It was shown that simple metal salts (CuCl, AgBF₄) or sterically undemanding complexes ($[(MeO)_3P-CuCl]$) yielded only insoluble grayish or poorly soluble violet solids, that defy characterization.

Desirable properties such as high stability, solubility, light-fastness, and fluorescence of the complexes depend, in most cases, on the metal center. In that respect it turned out that the gold complexes **6a–f**, **7c**, and **8c** exceed any other derivative. But the influence of the ligands L and the phenyl groups R^1 must not be ignored: for example, **7c** with $L = PEt_3$ is obtained in good yield and has good solubility in common organic solvents, however it decomposes in chloroform within minutes. The use of the isonitrile ligand CNtBu in **8c** appeared to be a good compromise, combining high fluorescence quantum yields with good stability and solubility in common organic solvents. However it decomposes in the presence of alcohols and amines and is obtained in low yield, usually 12%. Additionally, the substituents on the phenyl groups of the DPP core have a remarkable effect on the solubility: among **6a–d** ($R^1 = para-C_6H_4X; X = H, Me, Cl, \text{ and } CN$), derivative **6c** with chlorine is by far the least soluble.

The above-mentioned lack of stability of the dissolved copper and silver complexes **4a,c** and **5a,c**, respectively, can essentially be attributed to the high polarities of the metal–nitrogen bonds, which are therefore easy to cleave. Furthermore, two experiments indicate a stepwise dissociation of PPh₃. First, the addition of $[(CO)_4Cr(NCCH_3)_2]$ to a solution of **4c** resulted in a red precipitate, which is assumed to consist of “DPPCu₂”, according to IR spectral and elemental analyses. IR and ³¹P{¹H} NMR spectra of the yellow solution confirmed the presence of $[(CO)_4Cr(PPh_3)_2]$ (mixture of *cis* and *trans* isomers). Secondly, ³¹P{¹H} NMR measurements of compound **5c** at ambient temperature (not two doublets as expected, but one broad signal) and at –70 °C gave different

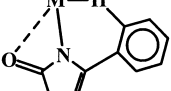
results (at least two similar species with Ag–PPh₃ bonds were detected in solution (CD₂Cl₂)). Consequently, an equilibrium with the monophosphane complex (like **6a–f**) can be formulated (see Scheme 3).

In contrast to the platinum complexes **10a,c**, the palladium derivatives **9a,c** are described best, according to elemental analyses, with only one PPh₃ ligand per metal center (i.e. a [(PPh₃)PdCl] fragment instead of [(PPh₃)₂PdCl]). Therefore the vacant coordination site makes it necessary to propose a μ -Cl bridged coordination polymer.

Molecular structures: Compounds **4c**, **5a**, **6b**, **c**, **e**, **7c**, and **8c** were obtained as single crystals suitable for X-ray crystal structure analyses by covering their solutions (CHCl₃ or CH₂Cl₂) with a layer of *n*-hexane or diethyl ether. Selected data of the structure determinations are compared in Table 1, and the molecular structures themselves are presented in Figure 1, Figure 2, Figure 3, Figure 4, Figure 5, Figure 6, and Figure 7. Selected bond lengths and angles are given in the captions. In all cases, the complexes are symmetrical to inversion, and either metal is linked to the lactam nitrogen of the planar DPP skeleton.

In **4c** and **5a**, the copper and silver atoms, respectively, are surrounded in a trigonal planar arrangement by one N and two P atoms (sum of angles = 360° (**4c**) and 357° (**5a**)). The

Table 1. Selected structural data of DPP complexes for comparison.^[a]

	M–N [pm]	M...O [pm]	M...H [pm]	DPP–Ph [°]	M–N–DPP [°]
					
4c	198	305	270	25	18
5a	224	277	281	4.5	15
6b	204	301	252	8	1
6c	205	305	239	1.5	3
6e	205	320	272	21	18
7c	206	318	277	27	16
8c	204/204	313/304	261/251	28/8	4/12.5

[a] Calculated van der Waals radii for M...O and M...H, respectively: M = Cu: 290 and 280; M = Ag: 320 and 310; M = Au: 320 and 310 pm.

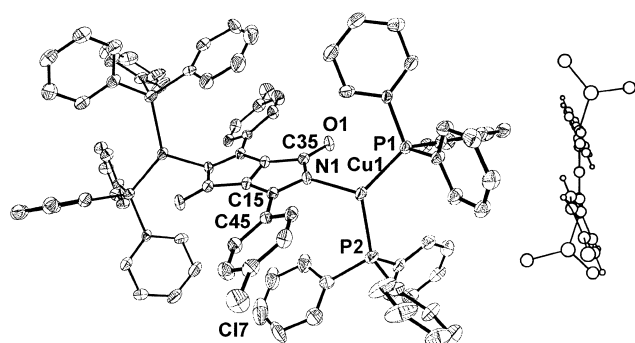


Figure 1. Molecular structure of **4c**. Principal bond lengths [pm] and angles [°]: Cu1–N1 198.4(5), Cu1–P1 222.9(2), Cu1–P2 225.3(2), O1–C35 123.8(8), N1–C15 134.1(8), N1–C35 139.6(8), C15–C45 147.8(9); N1–Cu1–P1 118.68(15), N1–Cu1–P2 113.74(16), P1–Cu1–P2 127.48(7), C15–N1–C35 110.7(5), C15–N1–Cu1 130.6(4), C35–N1–Cu1 114.2(4), N1–C15–C45 122.1(5), O1–C35–N1 124.6(6); sum of angles at N: 355.52; sum of angles at Cu: 360.

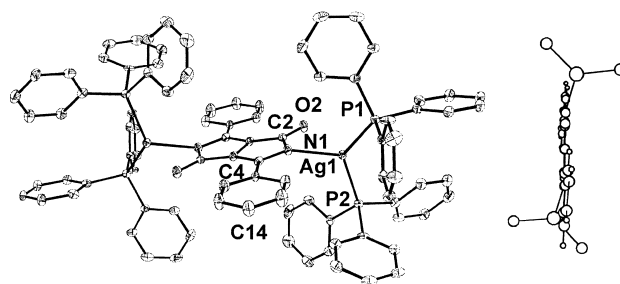


Figure 2. Molecular structure of **5a**. Principal bond lengths [pm] and angles [°]: Ag1–N1 224.2(5), Ag1–P1 240.96(19), Ag1–P2 243.3(2), N1–C4 135.4(8), N1–C2 137.5(8), C2–O2 123.7(8), C4–C14 146.3(9); N1–Ag1–P1 115.64(15), N1–Ag1–P2 112.49(16), P1–Ag1–P2 128.87(7), C4–N1–C2 110.1(5), C4–N1–Ag1 145.3(5), C2–N1–Ag1 101.3(4), O2–C2–N1 122.7(6), N1–C4–C14 123.0(6); sum of angles at N: 356.77; sum of angles at Ag: 356.99.

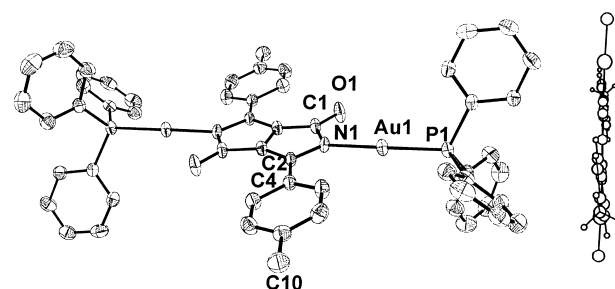


Figure 3. Molecular structure of **6b**. Principal bond lengths [pm] and angles [°]: Au1–N1 204.4(5), Au1–P1 222.7(4), O1–C1 124.3(6), N1–C2 139.1(9), N1–C1 139.5(9), C2–C4 146.7(1); N1–Au1–P1 176.9(9), C2–N1–C1 109.5(5), C2–N1–Au1 135.3(0), C1–N1–Au1 115.21, O1–C1–N1 120.8(6), N1–C2–C4 122.6(6); sum of angles at N: 359.96.

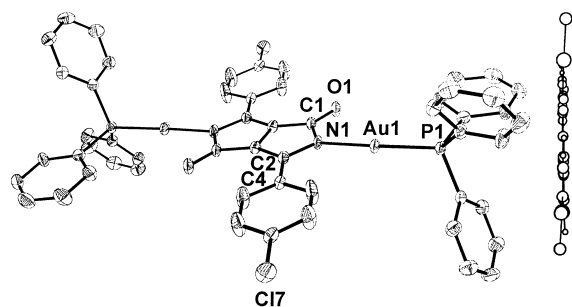


Figure 4. Molecular structure of **6c**. Principal bond lengths [pm] and angles [°]: Au1–N1 204.7(5), Au1–P1 223.0(2), O1–C1 124.7(8), N1–C2 138.3(9), N1–C1 139.5(9), C2–C4 146.7(10); N1–Au1–P1 175.3(2), C2–N1–C1 110.0(5), C2–N1–Au1 134.1(5), C1–N1–Au1 115.8(4), O1–C1–N1 122.2(6), N1–C2–C4 123.2(6); sum of angles at N: 359.92.

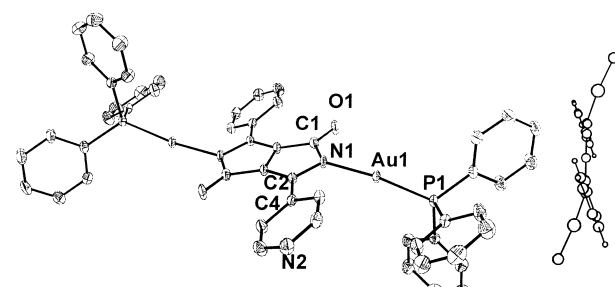


Figure 5. Molecular structure of **6e**. Principal bond lengths [pm] and angles [°]: Au1–N1 204.5(4), Au1–P1 224.04(13), O1–C1 122.1(6), N1–C2 138.4(6), N1–C1 141.7(6), C2–C4 146.6(7); N1–Au1–P1 172.34(12), C2–N1–C1 109.5(4), C2–N1–Au1 128.1(2), C1–N1–Au1 118.5(3), O1–C1–N1 122.8(8), N1–C2–C4 123.0(4); sum of angles at N: 356.10.

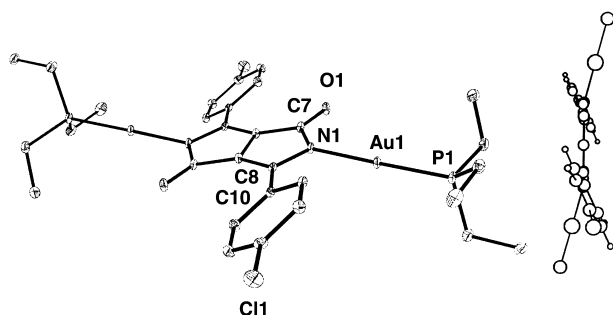


Figure 6. Molecular structure of **7c**. Principal bond lengths [pm] and angles [°]: Au1–N1 205.7(3), Au1–P1 224.09(10), N1–C8 138.2(4), N1–C7 140.3(5), O1–C7 123.0(4), C8–C10 146.1(5); N1–Au1–P1 178.37(9), C8–N1–C7 109.6(3), C8–N1–Au1 129.7(3), C7–N1–Au1 118.1(2), O1–C7–N1 123.3(3), N1–C8–C10 122.6(3); sum of angles at N: 357.48.

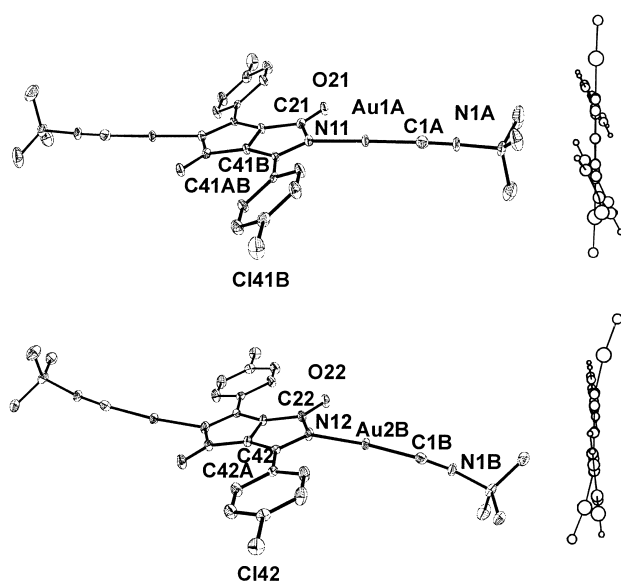


Figure 7. Molecular structure of **8c** (two different molecules). Principal bond lengths [pm] and angles [°]: Au1A–C1A 194.4(7), Au1A–N11 203.5(5), Au2B–C1B 195.4(7), Au2B–N12 204.2(5), C1A–N1A 113.9(8), N1A–C2A 146.3(8), N11–C41 137.8(7), N11–C21 138.7(8), C21–O21 124.0(7), C1B–N1B 112.5(7), N1B–C2B 147.6(7), N12–C42 137.8(7), N12–C22 139.1(8), C22–O22 123.9(7); C1A–Au1A–N11 177.6(3), C1A–Au1A–Au2B 96.6(2), N11–Au1A–Au2B 85.06(16), C1B–Au2B–N12 171.9(3), C1B–Au2B–Au1A 92.0(2), N12–Au2B–Au1A 95.50(17), N1A–C1A–Au1A 177.1(7), C1A–N1A–C2A 175.2(7), C41–N11–Au1A 131.5(4), C21–N11–Au1A 117.5(4), O21–C21–N11 124.5(5), N1B–C1B–Au2B 174.3(7), C1B–N1B–C2B 171.0(7), C42–N12–Au2B 132.2(4), C22–N12–Au2B 114.5(4), O22–C22–N12 122.7(5), N12–C42–C42A 124.7(5); sum of angles at N11: 359.99; sum of angles at N12: 358.34.

small deviation from planarity in **5a** is caused by a weak bonding interaction of Ag to the neighboring lactam oxygen (Ag...O = 277 pm, van der Waals radius = 320 pm). The M–N bond lengths differ due to the differing ionic radii of M from 198 pm (**4c**) to 224 pm (**5a**). The metal atoms are forced out-of-plane by 18° (**4c**) and 15° (**5a**). The P₂M planes and the planes of the rings R¹ are twisted by 70° and 25° (**4c**) and 85° and 5° (**5a**), respectively, with respect to the central plane of the DPP moiety. This indicates the enormous steric demand of the 12 surrounding phenyl groups.

The gold atoms in the DPP complexes are linearly coordinated (N–Au–L = 172–180°, L = PPh₃, PET₃, CN*t*Bu)

to one N and one P (**6b**, **c**, **e**, and **7c**) or one C atom (**8c**), respectively. Linear gold complexes of a similar type with biologically active ligands were reported by Beck et al.^[8] The sterically less demanding gold–DPP complexes leave enough space for the planarization of R¹ into the plane of the central chromophore. The gold atoms are forced out-of-plane by a minimum of about 1° (**6b,c**) to a maximum value of 18° (**6e**). The planes of the arene groups R¹ are twisted from only 1° (**6b,c**) up to 28° (**8c**) with respect to the chromophore plane. The distances Au–N are found to be in the range of about 205 pm, and the Au–P distances are about 223 pm.

It is noteworthy that in the solid state the gold complexes **6b,c** have very short Au...H distances of about 260 pm, which remain significantly below the calculated van der Waals radii of 310 pm. There is, however, no evidence for agostic bonds between Au and H. At ambient temperature, ¹H NMR spectra of **6b,c** only show two groups of signals. This indicates an AA'BB' spin system but not the expected ABCD spin system, in which four groups of signals should be found. Obviously, magnetic properties of both *ortho*- and both *meta*-phenyl protons are equivalent by a fast rotation (compared with the NMR timescale) of the phenyl groups in solution.

The isonitrile complex **8c** offers a special feature: the small steric demand of the *t*BuNC ligands enables intermolecular d¹⁰–d¹⁰ interactions between Au^I centers of different molecules. In the resulting coordination polymer, each Au^I center of one molecule is connected to another one of two different neighboring molecules, leading to infinite chains throughout the crystal (see Figure 8). The Au1A–Au2B distance is 311.68(6) pm, and two adjacent molecules are arranged almost coplanar to each other and are twisted by a torsion angle N11–Au1A–Au2B–N12 of about 150°. The unit cell of **8c** contains two different molecular structures of **8c**. Whereas one is perfectly linear, the other is somewhat bent in an S-shaped manner; both molecules alternate in the chain arrangement.

Absorption and fluorescence: All measurements were carried out in solution (CHCl₃; CH₂Cl₂ if necessary) at ambient temperature. Dye **1** (R¹ = 3,5-di-*t*BuC₆H₃, R = H) was used as a reference for the UV/Vis spectra of **4–10**, because of its sufficiently high solubility caused by the four *tert*-butyl groups.^[9] It exhibits a structured UV/Vis absorption spectrum (λ_{max} = 507 nm) and a mirror-type fluorescence spectrum (λ_{max} = 513 nm, see Figure 9). In the analogous *N*-methylated dye **3** (R¹ = 3,5-di-*t*BuC₆H₃, R = Me), blocking of the hydrogen bonds leads to a higher fluorescence quantum yield and a hypsochromic shift of the absorption maximum (λ_{max} = 486 nm, Figure 9, fluorescence: λ_{max} = 525 nm). However, blocking the N atoms with a metal complex, for example, AuPPh₃ in **6c**, results in a higher fluorescence quantum yield and, in contrast to the N–Me derivative **3**, in a bathochromic shift (absorption: λ_{max} = 537 nm; fluorescence: λ_{max} = 561 nm). Measured λ_{max} values of selected metalated dyes are given in Table 2. It demonstrates a significant influence of the metals M, their ligands L_n, and the substituents R¹. The bathochromic shift is the main change in the UV/Vis spectra and is caused by a high negative partial charge in **4–10**, which still remains

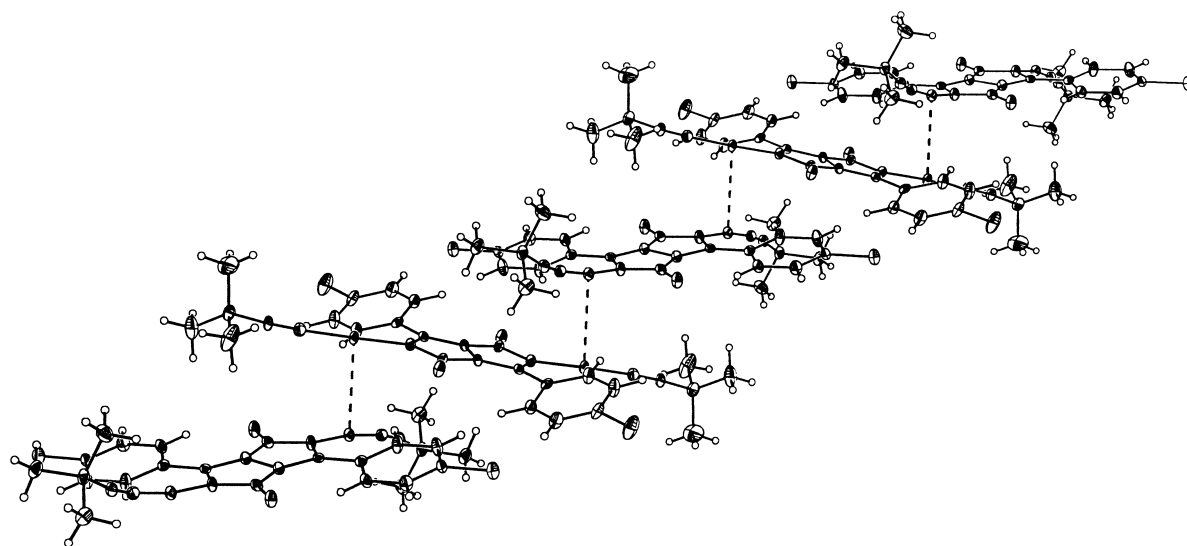


Figure 8. Coordination polymers of **8c**. Principal bond lengths [pm] and angles [°]: intermolecular $d^{10}-d^{10}$ interaction: Au1A–Au2B 311.68(6); chain arrangement by N–Au–Au–N torsion: N11–Au1A–Au2B–N12 –150.6(2). Distorted S-shaped and perfectly linear molecules alternate in the chain.

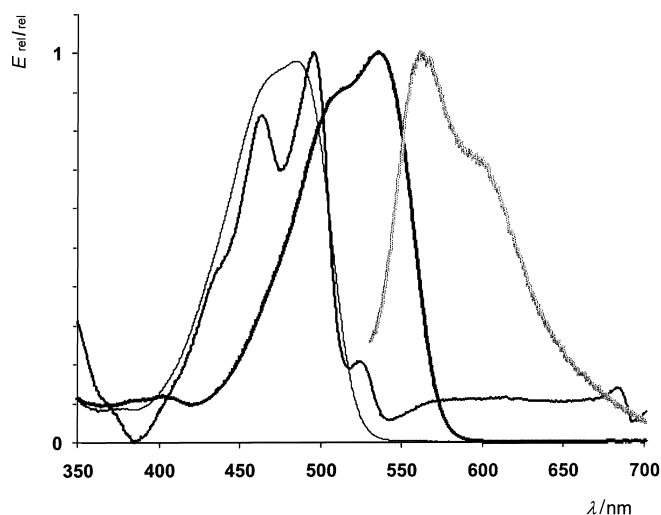


Figure 9. UV/Vis absorption and fluorescence spectrum of **6c** (thick black line, gray line), absorption spectra of **1** ($R' = 3,5$ -di-*t*BuC₆H₃, medium black line), and the *N*-methyl analogue **3** (thin black line) in CHCl₃.

after complexation of the dianion **2**. This is confirmed by IR spectroscopy: $\nu(\text{CO})$ of the lactam unit is lowered from typically 1640 cm^{−1} (**1**) to 1620 cm^{−1} (**6–8**) or even 1590 cm^{−1} (**4a,c**, **5a,c**). Thus the increased donor strength of the lactam nitrogen, that is, the now energetically higher lying HOMO, diminishes the HOMO–LUMO gap. Following the increasing polarity of the M–N bond (M = Au → Cu), λ_{max} increases

Table 2. Influence of metals M, ligands L, and aryl substituents R¹ on λ_{max} in the absorption spectra of selected DPP complexes.

M	Cu (4c)	Ag (5c)	Au (6c)	
λ_{max} [nm]	572	562	537	
L	PEt ₃ (7c)	PPh ₃ (6c)	CN <i>t</i> Bu (8c)	
λ_{max} [nm]	550	537	536	
R ¹	C ₆ H ₄ –CN (6d)	C ₆ H ₄ –Cl (6c)	C ₆ H ₅ (6a)	C ₆ H ₄ –CH ₃ (6b)
λ_{max} [nm]	576	537	530	526

in the order **6a–f** → **5a,c** → **4a,c** by steps of about 20 nm. Electron-donating ligands L_n at the gold center show a similar influence on the shift of λ_{max} (L_n = PPh₃ (**6c**), PEt₃ (**7c**); λ_{max} = 537, 550 nm) as do electron-withdrawing groups in the *para*-position of the phenyl substituents R¹ = C₆H₃–X in compounds **6** (**6a**: 530; **6b**: 526; **6c**: 537; **6d**: 576 nm).

The measurements of the emission lifetime of the dye complexes (excitation at 520 nm) show a monoexponential dying-out of the fluorescence; that means there are no concurrent processes such as ISC (intersystem crossing) or phosphorescence. The lifetimes of the S₁ levels of **5a**, **6c**, **8c**, and **10c** are given in Table 3 with values similar to those of the unmetallated dyes.

Table 3. Emission lifetimes of some DPP complexes (in CHCl₃, **5a** in CH₂Cl₂; error limit in parenthesis).

	5a	6c	8c	10c
τ [ns]	8.02 (±0.01)	6.70 (±0.05)	6.56 (±0.05)	5.21 (±0.01)

The previously mentioned dissociation process especially for M = Cu, Ag (**4a,c**, **5a,c**; Scheme 3) does not affect their UV/Vis spectra, hence those of **5a,c** resemble those of **6a–f**. However, the characteristic shape of the main absorption of **4c** leads us to the conclusion, that two independent absorption maxima at 548 and 572 nm are superimposed. Excitation at 520 nm, which is expected to excite the species with the absorption maximum at 548 nm alone, results in an emission band with λ_{max} about 560 nm (Figure 10). Irradiation at 572 nm, however, which could prove this assumption, was not possible for technical reasons. Besides these main absorptions, another band between 400–450 nm can be excited to fluoresce at about 510 nm. A similar band also exists in the spectra of the palladium (**9a,c**) and platinum (**10a,c**) complexes. The coupling patterns in the ³¹P NMR spectra of **10a,c** confirm nonfluxional behavior (two sharply resolved doublets), so it is more reasonable to assign the

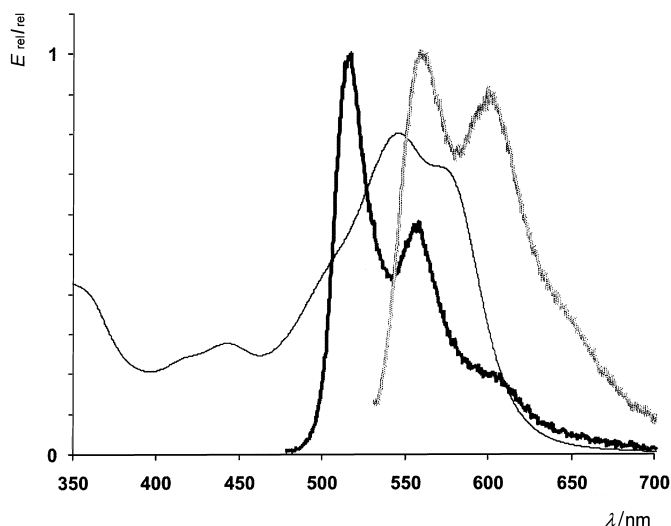


Figure 10. UV/Vis absorption spectrum (thin black line) and fluorescence spectra of **4a** in CH_2Cl_2 at two excitation energies (455 nm: thick black line; 520 nm: gray line).

absorption at 400–450 nm as an additional band of a single molecule.

As mentioned above, the fluorescence quantum yield of **1a** was found to be 50 %, and N-alkylation (**3a**) increases it only by a few percent. Since the DPP dianions do not fluoresce or if so then poorly, we expected to observe very much the same when they are attached to any other (d-)metal center. As expected, complexation with copper (**4a,c**) decreases the quantum yield to about 20 %. Surprisingly high fluorescence quantum yields, over 80 %, are measured for the silver (**5a,c**) and gold (**6a–f**, **7c**, **8c**) complexes. Values up to 100 % are found for **6a,c**. The influence of relativistic effects might seem a reasonable explanation. However, this argument is mitigated by the fact, that fluorescence quantum yields measured for the platinum complexes **10a,c** are far below expectations: only 15 %. Fluorescence in the corresponding palladium complexes **9a,c** was quenched to an indeterminable level. Furthermore, the fluorescence behavior does not depend solely on the absorption range: although **5c** (562 nm) and **10c** (554 nm) show similar λ_{max} values, their fluorescence quantum yields differ significantly (**5c**: $\Phi = 85$ %; **10c**: $\Phi = 13$ %).

The fluorescence quantum yields correlate with the Stokes shifts: they increase when the latter decrease, with **6f** and **7c** as the only exceptions (Figure 11). Interestingly there is a second correlation between the fluorescence quantum yield (measured in solution) and the torsion angle (solid state) DPP– R^1 (Figure 12). Thus, in **6c** with one of the highest fluorescence quantum yields ($\Phi \approx 100$ %), both the torsion angle DPP– R^1 (1.5°) and the Stokes shift (24 nm) are among the smallest of the gold-containing derivatives. The substituents R^1 in the other complexes are all rotated to a larger extent from planarity.

It should be taken into account, that DPP dyes are assumed to undergo planarization after excitation.^[6] According to this and with respect to the available data, it seems sensible to relate high fluorescence quantum yields in DPP complexes to the ease of minimizing the torsion angle DPP– R^1 during

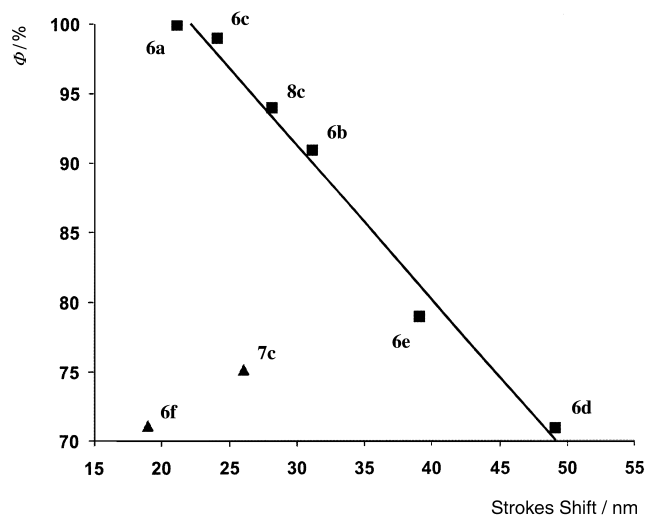


Figure 11. Correlation of fluorescence quantum yields with Stokes shifts in DPP complexes (■). Two complexes with less fluorescence deviate from the line of best fit (▲).

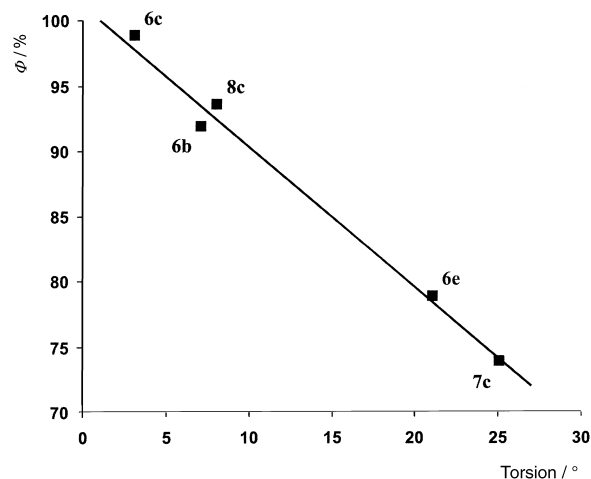


Figure 12. Correlation of fluorescence quantum yields with torsion angles DPP– R^1 in DPP complexes (only one molecule of **8c**).

excitation. If this process is impeded, as can be estimated by the angles DPP– R^1 found by X-ray structure determination, more energy is needed for this, and the fluorescence quantum yields are diminished.

Experimental Section

All reactions were performed by using Schlenk techniques under an atmosphere of Ar in dry and argon-saturated solvents.^[10] The starting materials $[(\text{Ph}_3\text{P})\text{AuCl}]$,^[11] $[(\text{Et}_3\text{P})\text{AuCl}]$,^[11] $[(t\text{BuNC})\text{AuCl}]$,^[7] and $[(\text{Ph}_3\text{P})_2\text{PtCl}_2]$ ^[12] were prepared as described in the literature. The DPP dyes **1a–f** were made available by the groups of Prof. Dr. H. Langhals and Prof. Dr. R. Gompper (†). The other reagents were purchased from Sigma-Aldrich, Strem, or Fluka. Elemental analyses were performed by the Analytical Laboratory of the Department of Chemistry of the University of Munich. Infrared spectra were recorded on Nicolet 520FT-IR, NMR spectra on Jeol 6SX270 (internal SiMe_4 as standard, 20°C), UV/Vis absorption spectra on Bonin Instruments Omega2000, and fluorescence spectra on Perkin Elmer 3000 instruments. The perylene dye S-13^[3] was used as a reference for the fluorescence quantum yield determination. Varian MAT711A and Jeol MS700 were used for the recording of mass

spectra. Crystallographic data were collected with Spellman DF4 Series, Nonius CAD4, and Nonius Mach3 instruments.

General procedure: Addition of $[\text{Na}(\text{SiMe}_3)_2]$ (0.30 mL, 1 molar solution in THF) to a well-stirred solution of the DPP derivatives **1a–f** (40 (**a**), 44 (**b**), 50 (**c**), 47 (**d**), 41 (**e**), and 42 mg (**f**) = 0.14 mmol) in DMF (10 mL) yielded blue solutions of **2a–f**, which were used in all following reactions. They were added dropwise to a stirred solution of $[\text{L}_m\text{MX}]$ (0.30 mmol) in DMF (5 mL) at ambient temperature and left stirring for two further hours. The purification is given below.

Complexes 4a,c: $[\text{L}_m\text{MX}] = [(\text{Ph}_3\text{P})_2\text{CuNO}_3]$ (195 mg). The solvent was removed under reduced pressure at 60 °C, and the resulting residue was dissolved in CHCl_3 (10–15 mL) and filtered (P3). The solution was carefully diluted with *n*-hexane (20 mL) and stored at –20 °C for some days. To improve the yield, the solution can be layered with some more mL of *n*-hexane. Compound **4a** was only formed as microcrystalline solid, whereas **4c** precipitated as violet crystals.

Compound 4a: Yield 102 mg (46 %), violet solid, m.p. 143 °C; IR (KBr): $\tilde{\nu} = 3061, 1698, 1644, 1610, 1569, 1498, 1481, 1456, 1435, 1351, 1328, 1266, 1202, 1147, 1097, 1073, 1027, 1000, 815, 771, 743, 698, 661, 526, 517, 506, 493, 440, 335 \text{ cm}^{-1}$; ^1H NMR (270 MHz, CDCl_3): $\delta = 7.17\text{--}7.32$ (m; PPh_3 , DPP–Ph); $^{31}\text{P}\{^1\text{H}\}$ NMR (109.4 MHz, CDCl_3): $\delta = -3.5$ (s; PPh_3); FAB-MS: m/z : 676 $[\text{M}^+ - 3\text{PPh}_3]$, 587 $[\text{Cu}(\text{PPh}_3)_2]$; UV/Vis (CH_2Cl_2): λ_{max} (ϵ_{rel}) = 533 (1.0), 565 nm (0.9); fluorescence (CH_2Cl_2): λ_{max} (I_{rel}) = 557 (1.0), 597 nm (0.95); $\Phi = 22\%$; elemental analysis calcd (%) for $\text{C}_{90}\text{H}_{70}\text{Cu}_2\text{N}_2\text{O}_2\text{P}_4 \cdot \text{CHCl}_3$ (1581.9): C 69.09, H 4.49, N 1.77; found: C 69.46, H 4.86, N 2.14.

Compound 4c: Yield 111 mg (42 %), violet crystals, m.p. 165 °C; IR (KBr): $\tilde{\nu} = 3075, 3035, 1607, 1598, 1579, 1556, 1521, 1481, 1435, 1408, 1342, 1300, 1277, 1262, 1214, 1182, 1157, 1121, 1093, 1070, 1027, 1011, 998, 837, 828, 820, 773, 741, 694, 642, 628, 618, 527, 516, 507, 490, 442, 431 \text{ cm}^{-1}$; ^1H NMR (270 MHz, CDCl_3): $\delta = 7.15\text{--}7.37$ (m; PPh_3 , DPP– $\text{C}_6\text{H}_4\text{Cl}$); $^{31}\text{P}\{^1\text{H}\}$ NMR (109.4 MHz, CDCl_3): $\delta = -2.4$ (s; PPh_3); FAB-MS: m/z : 1007 $[\text{M}^+ - 2\text{PPh}_3]$, 587 $[\text{Cu}(\text{PPh}_3)_2]$; UV/Vis (CH_2Cl_2): λ_{max} (ϵ_{rel}) = 548 (1.0), 572 nm (0.9); fluorescence (CH_2Cl_2): λ_{max} (I_{rel}) = 562 (1.0), 609 nm (0.75); $\Phi = 20\%$; solid-state fluorescence: λ_{max} = 642 nm; elemental analysis calcd (%) for $\text{C}_{90}\text{H}_{68}\text{Cl}_2\text{Cu}_2\text{N}_2\text{O}_2\text{P}_4 \cdot 4\text{CHCl}_3$ (1889.5): C 54.93, H 3.52, N 1.33; found: C 55.49, H 3.66, N 1.46.

Complexes 5a,c: $[\text{L}_m\text{MX}] = \text{AgBF}_4$ (58 mg) and 3 equiv PPh_3 (236 mg, 0.90 mmol). Compounds **5a,c** precipitated as violet solids. The solvent was removed, and the residue washed with acetone (25 mL, three times) and diethyl ether (25 mL) and dried in vacuo.

Compound 5a: This was dissolved in CH_2Cl_2 (15 mL), filtered (P3), layered with *n*-hexane (25 mL), and stored at 0 °C. Compound **5a** precipitated as thin, red crystals; yield 137 mg (63 %), red platelets, m.p. 210 °C; IR (KBr): $\tilde{\nu} = 3069, 3053, 1580, 1558, 1519, 1481, 1446, 1435, 1350, 1333, 1308, 1288, 1232, 1215, 1180, 1155, 1124, 1095, 1073, 1025, 997, 923, 821, 767, 743, 694, 665, 648, 617, 513, 504, 493, 438, 336 \text{ cm}^{-1}$; ^1H NMR (270 MHz, CDCl_3): $\delta = 7.15\text{--}7.45$ (m; PPh_3 , DPP–Ph); $^{31}\text{P}\{^1\text{H}\}$ NMR (109.4 MHz, CDCl_3): $\delta = 8.3$ (s; PPh_3); FAB-MS: m/z : 1027 $[\text{M}^+ - 2\text{PPh}_3]$, 631 $[\text{Ag}(\text{PPh}_3)_2]$; UV/Vis (CH_2Cl_2): λ_{max} (ϵ_{rel}) = 550 (1), 515 nm (0.8); fluorescence (CH_2Cl_2): λ_{max} (I_{rel}) = 565 (1.0), 600 nm (0.8); $\Phi = 83\%$; solid-state fluorescence: λ_{max} = 642 nm; elemental analysis calcd (%) for $\text{C}_{90}\text{H}_{70}\text{Ag}_2\text{N}_2\text{O}_2\text{P}_4$ (1550.6): C 69.71, H 4.51, N 1.81; found: C 69.08, H 4.82, N 1.74.

Compound 5c: Soxhlet extraction of the crude product of **5c** with CH_2Cl_2 (200 mL) in the dark and covering the solution with a layer of *n*-hexane gave **5c** as a violet powder with small cubic crystals; yield 134 mg (59 %), violet solid, m.p. 223 °C; IR (KBr): $\tilde{\nu} = 3082, 3053, 1597, 1577, 1553, 1522, 1480, 1435, 1408, 1337, 1300, 1278, 1213, 1180, 1158, 1122, 1092, 1027, 1011, 998, 839, 818, 772, 743, 715, 694, 644, 630, 618, 513, 504, 490, 437 \text{ cm}^{-1}$; ^1H NMR (270 MHz, CDCl_3): $\delta = 7.15\text{--}7.45$ (m; PPh_3 , DPP– $\text{C}_6\text{H}_4\text{Cl}$); $^{31}\text{P}\{^1\text{H}\}$ NMR (109.4 MHz, CDCl_3): $\delta = 8.5$ (s; PPh_3); FAB-MS: m/z : 1096 $[\text{M}^+ - 2\text{PPh}_3]$, 631 $[\text{Ag}(\text{PPh}_3)_2]$; UV/Vis (CH_2Cl_2): λ_{max} (ϵ_{rel}) = 560 (1.0), 526 nm (0.8); fluorescence (CH_2Cl_2): λ_{max} (I_{rel}) = 572 (1.0), 615 nm (0.8); $\Phi = 85\%$; solid-state fluorescence: λ_{max} = 665 nm; elemental analysis calcd (%) for $\text{C}_{90}\text{H}_{68}\text{Ag}_2\text{Cl}_2\text{N}_2\text{O}_2\text{P}_4 \cdot 1\text{CH}_2\text{Cl}_2$ (1704.8): C 64.10, H 4.11, N 1.64; found: C 65.09, H 4.27, N 1.93.

Complexes 6a–f: $[\text{L}_m\text{MX}] = [(\text{Ph}_3\text{P})\text{AuCl}]$ (148 mg).

Compound 6a precipitated after addition of water (20 mL). The crude product was filtered (P3) and dried in vacuo. Dissolving in CH_2Cl_2 (10 mL)

and layering with *n*-hexane yielded a red solid; yield 163 mg (95 %), red solid, m.p. 251 °C; IR (KBr): $\tilde{\nu} = 3436, 3053, 1814, 1612, 1557, 1487, 1436, 1344, 1330, 1310, 1202, 1183, 1160, 1117, 1102, 1074, 1026, 998, 917, 829, 794, 748, 734, 711, 692, 544, 509 \text{ cm}^{-1}$; ^1H NMR (400 MHz, CDCl_3): $\delta = 7.47\text{--}7.60$ (m, 40H; Ph); $^{31}\text{P}\{^1\text{H}\}$ NMR (162 MHz, CDCl_3): $\delta = 28.4$ (s; PPh_3); FAB-MS: m/z : 1205 $[\text{M}^+]$, 459 $[\text{Au}(\text{PPh}_3)_3]$; UV/Vis (CHCl_3): λ_{max} (ϵ) = 530 nm (20 400); fluorescence (CHCl_3): λ_{max} = 536 nm; $\Phi = 100\%$; solid-state fluorescence: λ_{max} = 608 nm; elemental analysis calcd (%) for $\text{C}_{54}\text{H}_{40}\text{Au}_2\text{N}_2\text{O}_2\text{P}_2 \cdot \text{H}_2\text{O}$ (1222.8): C 53.04, H 3.46, N 2.29; found: C 53.07, H 3.41, N 2.31.

Compounds **6b,d–f** precipitated after addition of diethyl ether (60 mL). The products were filtered (P3), dried, and washed with diethyl ether and *n*-hexane. Purple to violet solids were obtained by layering solutions of **6b,d–f** in CHCl_3 (10 mL) with diethyl ether.

Compound 6b: Yield 102 mg (59 %), red solid, m.p. 271 °C; IR (KBr): $\tilde{\nu} = 3436, 3051, 3013, 2919, 2855, 1609, 1503, 1481, 1436, 1335, 1310, 1190, 1102, 1027, 997, 825, 748, 710, 694, 544, 510 \text{ cm}^{-1}$; ^1H NMR (400 MHz, CDCl_3): $\delta = 8.67$ (d, $^3J = 8.1 \text{ Hz}$, 4H; DPP–CCH), 7.60 (ddd, $^3J(\text{H,H}) = 13.0$, $^3J(\text{H,H}) = 6.8$, $^4J(\text{H,H}) = 1.6 \text{ Hz}$, 12H; *o*-Ph), 7.52–7.50 (m, 6H; *p*-Ph), 7.48–7.45 (m, 12H; *m*-Ph), 7.12 (d, $^3J(\text{H,H}) = 8.1 \text{ Hz}$, 4H; DPP–CCHCH), 2.35 (s, 6H; CH_3); $^{31}\text{P}\{^1\text{H}\}$ NMR (162 MHz, CDCl_3): $\delta = 28.6$ (s; PPh_3); FAB-MS: m/z : 1233 $[\text{M}^+ - 1]$, 1232 $[\text{M}^+]$, 774 $[\text{M}^+ - \text{Au}(\text{PPh}_3)]$, 459 $[\text{Au}(\text{PPh}_3)_3]$; UV/Vis (CHCl_3): λ_{max} (ϵ) = 525 nm (22 900); fluorescence (CHCl_3): λ_{max} = 557 nm; $\Phi = 92\%$; solid-state fluorescence: λ_{max} = 661 nm; elemental analysis calcd (%) for $\text{C}_{54}\text{H}_{44}\text{Au}_2\text{N}_2\text{O}_2\text{P}_2$ (1232.8): C 54.56, H 3.60, N 2.27; found: C 54.19, H 3.55, N 2.29.

Compound 6d: Yield 84 mg (48 %), violet solid, m.p. 300 °C; IR (KBr): $\tilde{\nu} = 3436, 3054, 2924, 2222, 1623, 1600, 1495, 1481, 1436, 1411, 1334, 1307, 1286, 1190, 1102, 1028, 998, 918, 847, 745, 711, 694, 544, 504 \text{ cm}^{-1}$; ^1H NMR (400 MHz, CDCl_3): $\delta = 8.86$ (d, $^3J(\text{H,H}) = 8.6 \text{ Hz}$, 4H; NCCCH), 7.47–7.57 (m, 34H; Ph, NCCCHCH); $^{31}\text{P}\{^1\text{H}\}$ NMR (162 MHz, CDCl_3): $\delta = 28.1$ (s; PPh_3); FAB-MS: m/z : 1255 $[\text{M}^+]$, 459 $[\text{Au}(\text{PPh}_3)_3]$; UV/Vis (CHCl_3): λ_{max} (ϵ) = 576 nm (23 900); fluorescence (CHCl_3): λ_{max} = 625 nm; $\Phi = 71\%$; solid-state fluorescence: λ_{max} = 750 nm; elemental analysis calcd (%) for $\text{C}_{56}\text{H}_{38}\text{Au}_2\text{N}_4\text{O}_2\text{P}_2$ (1254.8): C 53.60, H 3.05, N 4.46; found: C 53.25, H 3.09, N 4.56.

Compound 6e: Yield 91 mg (50 %), red solid, m.p. 266 °C; IR (KBr): $\tilde{\nu} = 3436, 3054, 2928, 1630, 1586, 1566, 1531, 1480, 1435, 1414, 1346, 1313, 1220, 1196, 1102, 1068, 997, 827, 745, 710, 693, 544, 510 \text{ cm}^{-1}$; ^1H NMR (400 MHz, CDCl_3): $\delta = 8.63$ (dd, $^3J(\text{H,H}) = 6.2$, $^5J(\text{H,H}) = 1.6 \text{ Hz}$, 4H; NCH), 8.57 (dd, $^3J(\text{H,H}) = 6.2$, $^5J(\text{H,H}) = 1.6 \text{ Hz}$, 4H; NCHCH), 7.47–7.60 (m, 30H; Ph); $^{31}\text{P}\{^1\text{H}\}$ NMR (162 MHz, CDCl_3): $\delta = 28.4$ (s; PPh_3); FAB-MS: m/z : 1206 $[\text{M}^+]$, 459 $[\text{Au}(\text{PPh}_3)_3]$; UV/Vis (CHCl_3): λ_{max} (ϵ) = 557 nm (17 100); fluorescence (CHCl_3): λ_{max} = 596 nm; $\Phi = 79\%$; elemental analysis calcd (%) for $\text{C}_{52}\text{H}_{38}\text{Au}_2\text{N}_4\text{O}_2\text{P}_2 \cdot 0.75\text{CHCl}_3$ (1296.4): C 48.87, H 2.80, N 4.32; found: C 48.76, H 2.96, N 4.36.

Compound 6f: Yield 112 mg (66 %), violet solid, m.p. 266 °C; IR (KBr): $\tilde{\nu} = 3436, 3072, 3054, 2924, 1614, 1555, 1504, 1481, 1436, 1377, 1298, 1234, 1182, 1123, 1102, 1055, 1027, 998, 849, 740, 710, 693, 619, 543, 510 \text{ cm}^{-1}$; ^1H NMR (400 MHz, CDCl_3): $\delta = 9.03$ (dd, $^3J(\text{H,H}) = 3.6$, $^4J(\text{H,H}) = 1.5 \text{ Hz}$, 2H; DPP–CCH), 7.66 (ddd, $^3J(\text{H,H}) = 13$, $^3J(\text{H,H}) = 7.2$, $^4J(\text{H,H}) = 1.6 \text{ Hz}$, 12H; *o*-Ph), 7.52–7.49 (m, 18H; *m*-Ph), 7.13 (dd, $^3J(\text{H,H}) = 4.9$, $^4J(\text{H,H}) = 1.3 \text{ Hz}$, 2H; DPP–CCHCHCH), 7.11 (dd, $^3J(\text{H,H}) = 5.0$, $^4J(\text{H,H}) = 3.6 \text{ Hz}$, 2H; DPP–CCHCH); $^{31}\text{P}\{^1\text{H}\}$ NMR (162 MHz, CDCl_3): $\delta = 28.4$ (s; PPh_3); FAB-MS: m/z : 1216 $[\text{M}^+]$, 758 $[\text{M}^+ - \text{Au}(\text{PPh}_3)]$, 459 $[\text{Au}(\text{PPh}_3)_3]$; UV/Vis (CHCl_3): λ_{max} (ϵ) = 572 nm (31 900); fluorescence (CHCl_3): λ_{max} = 591 nm; $\Phi = 71\%$; elemental analysis calcd (%) for $\text{C}_{50}\text{H}_{36}\text{Au}_2\text{N}_2\text{O}_2\text{P}_2\text{S}_2$ (1216.9): C 49.35, H 2.98, N 2.30, S 5.27; found: C 48.81, H 2.85, N 2.35, S 5.13.

Compound **6c** precipitated as a red solid. The product was purified analogously to **5a**: it was dissolved in warm CHCl_3 (50 mL), filtered (P3), and layered with *n*-hexane to yield orange crystals; yield 136 mg (64 %), red to orange platelets, m.p. > 300 °C; IR (KBr): $\tilde{\nu} = 3082, 3053, 1699, 1673, 1615, 1574, 1484, 1436, 1405, 1330, 1302, 1277, 1200, 1183, 1119, 1102, 1092, 1027, 1011, 996, 836, 743, 711, 694, 545, 509, 484, 451, 440 \text{ cm}^{-1}$; ^1H NMR (270 MHz, CDCl_3): $\delta = 8.71$ (d, $^3J(\text{H,H}) = 8.62 \text{ Hz}$, 4H; DPP–CCHCH), 7.45–7.60 (m, 30H; Ph_3P), 7.26 (d, $^3J(\text{H,H}) = 8.88 \text{ Hz}$, 4H; DPP–CCH); $^{31}\text{P}\{^1\text{H}\}$ NMR (109.4 MHz, CDCl_3): $\delta = 33.01$ (s; PPh_3); $^{13}\text{C}\{^1\text{H}\}$ NMR (67.9 MHz, CDCl_3): $\delta = 170.7$ (s; C7), 152.4 (s; C5), 135.0 (s; C4), 134.3 (d, $^2J(\text{C,P}) = 14 \text{ Hz}$; *o*-Ph), 131.9 (d, $^4J(\text{C,P}) = 3 \text{ Hz}$; *p*-Ph), 131.45 (s; C1), 129.8 (s; C3), 129.3 (d, $^3J(\text{C,P}) = 12 \text{ Hz}$; *m*-Ph), 128.7 (d, $^1J(\text{C,P}) = 62 \text{ Hz}$; *i*Ph),

128.3 (s; C2); FAB-MS: m/z : 1274 [M^+], 814 [$M^+ - \text{Au}(\text{PPh}_3)$], 721 [$\text{Au}(\text{PPh}_2)_2$], 459 [$\text{Au}(\text{PPh}_3)$]; UV/Vis (CHCl_3): λ_{max} (ϵ) = 535 (26000), 513 nm (23400); fluorescence (CHCl_3): λ_{max} (I_{rel}) = 561 (1.0), 597 nm (0.7); Φ = 99%; solid-state fluorescence: λ_{max} = 633 nm; elemental analysis calcd (%) for $\text{C}_{54}\text{H}_{38}\text{Au}_2\text{Cl}_2\text{N}_2\text{O}_2\text{P}_2 \cdot 2\text{CHCl}_3$ (1512.4): C 44.72, H 2.66, N 1.86; found: C 43.91, H 2.67, N 1.93.

Compound 7c: [$L_n\text{MX}$] = [$(\text{Et}_3\text{P})\text{AuCl}$] (105 mg). The solvent was removed carefully at ambient temperature in vacuo. The residue was dissolved in CH_2Cl_2 (10 mL), and the solution filtered (P3), layered with *n*-hexane (50 mL), and stored at 0 °C to yield red crystals; yield 117 mg (78%), red crystals, m.p. 177 °C (decomp); IR (KBr): $\tilde{\nu}$ = 2967, 2931, 2901, 2873, 2170, 1675, 1645, 1616, 1486, 1456, 1410, 1384, 1331, 1262, 1164, 1103, 1092, 1063, 1044, 1013, 833, 798, 773, 761, 742, 707, 636, 484, 443, 312 cm^{-1} ; ^1H NMR (270 MHz, CDCl_3): δ = 8.69 (d, $^3J(\text{H,H})$ = 8.02 Hz, 4H; DPP–CCHCH), 7.35 (d, $^3J(\text{H,H})$ = 8.02 Hz, 4H; DPP–CCH), 1.84 (m, 12H; CH_2CH_3), 1.17 (m, 18H; CH_2CH_3); $^{31}\text{P}\{^1\text{H}\}$ NMR (109.4 MHz, CDCl_3): δ = 30.29 (s; PEt_3); FAB-MS: m/z : 670 [$M^+ - \text{Au}(\text{PEt}_3)$], 315 [$\text{Au}(\text{PEt}_3)$]; UV/Vis (CH_2Cl_2): λ_{max} (ϵ_{rel}) = 550 (1.0), 518 nm (0.8); fluorescence (CH_2Cl_2): λ_{max} (I_{rel}) = 576 (1.0), 615 nm (0.7); Φ = 74%; elemental analysis calcd (%) for $\text{C}_{30}\text{H}_{38}\text{Au}_2\text{Cl}_2\text{N}_2\text{O}_2\text{P}_2 \cdot \text{CH}_2\text{Cl}_2$ (1070.3): C 34.77, H 3.55, N 2.62; found: C 35.67, H 3.70, N 2.74.

Compound 8c: [$L_n\text{MX}$] = [$(t\text{BuNC})\text{AuCl}$] (95 mg). The solvent was removed carefully at ambient temperature in vacuo. The residue was dissolved in CHCl_3 (50 mL), and the solution filtered (P3), layered with *n*-hexane (50 mL), and stored at 0 °C to yield orange crystals; yield 17 mg (12%), red cubes, m.p. > 300 °C; IR (KBr): $\tilde{\nu}$ = 2988, 2959, 2923, 2851, 2233, 1722, 1622, 1594, 1575, 1548, 1487, 1406, 1373, 1335, 1304, 1278, 1263, 1235, 1202, 1190, 1120, 1108, 1093, 1012, 834, 815, 785, 741, 720, 540, 522, 485, 457 cm^{-1} ; ^1H NMR (270 MHz, CDCl_3): δ = 8.59 (d, $^3J(\text{H,H})$ = 8.91 Hz, 4H; DPP–CCHCH), 7.38 (d, $^3J(\text{H,H})$ = 8.88 Hz, 4H; DPP–CCH), 1.58 (s, 18H; $\text{C}(\text{CH}_3)_3$); $^{13}\text{C}\{^1\text{H}\}$ NMR (67.5 MHz, CDCl_3): δ = 208.2 (AuCN), 170.4, 152.2, 135.4, 130.8, 129.6, 128.4, 114.6, 59.1 ($\text{C}(\text{CH}_3)_3$), 29.8 ($\text{C}(\text{CH}_3)_3$); FAB-MS: m/z : 915 [M^+], 858 [$M^+ - t\text{Bu}$], 802 [$M^+ - 2t\text{Bu}$], 635 [$M^+ - \text{Au}(\text{CN}t\text{Bu})$]; UV/Vis (CHCl_3): λ_{max} (ϵ) = 536 (24800), 508 nm (21400);

fluorescence (CHCl_3): λ_{max} (I_{rel}) = 564 (1.0), 671 nm (0.7); Φ = 94%; solid-state fluorescence: λ_{max} (I_{rel}) = 628 (1.0), 683 nm (0.3); elemental analysis calcd (%) for $\text{C}_{28}\text{H}_{26}\text{Au}_2\text{Cl}_2\text{N}_4\text{O}_2 \cdot \text{CHCl}_3$ (1034.7): C 33.63, H 2.61, N 5.41; found: C 33.04, H 2.69, N 5.28.

Complexes 9a,c: [$L_n\text{MX}$] = PdCl_2 (53 mg) and 2 equiv PPh_3 (157 mg, 0.60 mmol). The solvent was removed under reduced pressure at 60 °C, and the residue dissolved in CH_2Cl_2 (15 mL) and filtered (P3). The solutions were layered with *n*-hexane (15 mL) and stored at 0 °C for 24 h. Compounds **9a,c** precipitated as fine, red powders.

Compound 9a: Yield 55%, brownish red powder, m.p. 180 °C (decomp); IR (KBr): $\tilde{\nu}$ = 3075, 3053, 1655, 1622, 1589, 1566, 1521, 1483, 1446, 1436, 1360, 1330, 1311, 1289, 1262, 1187, 1159, 1120, 1096, 1074, 1060, 1028, 999, 821, 745, 729, 707, 692, 617, 534, 520, 512, 496, 456, 334 cm^{-1} ; ^1H NMR (270 MHz, CDCl_3): δ = 7.79–7.27 (m, 60H; PPh_3); $^{31}\text{P}\{^1\text{H}\}$ NMR (109.4 MHz, CDCl_3): δ = 21.6 (s; PPh_3); FAB-MS: m/z : 952 [$M^+ - \text{PdCl}$], 690 [$M^+ - (\text{PPh}_3)\text{PdCl}$], 667 [$(\text{Ph}_3\text{P})_2\text{PdCl}$], 655 [$M^+ - (\text{PPh}_3)\text{PdCl}_2$]; UV/Vis (CHCl_3): λ_{max} (ϵ_{rel}) = 550 (1.0), 524 nm (0.9); elemental analysis calcd (%) for $\text{C}_{54}\text{H}_{40}\text{Cl}_2\text{N}_2\text{O}_2\text{P}_2\text{Pd}_2$ (1094.6): C 59.25, H 3.68, N 2.56; found: C 57.11, H 4.18, N 2.73.

Compound 9c: Yield 104 mg (64%), red to purple powder, m.p. > 300 °C; IR (KBr): $\tilde{\nu}$ = 3075, 3053, 1659, 1623, 1589, 1519, 1492, 1483, 1435, 1411, 1358, 1328, 1304, 1276, 1186, 1159, 1130, 1118, 1094, 1056, 1029, 1012, 999, 906, 837, 825 (m), 738, 708, 692, 619, 521, 512, 496, 456, 436, 340, 318 cm^{-1} ; ^1H NMR (270 MHz, CDCl_3): δ = 8.99 (d, $^3J(\text{H,H})$ = 8.32 Hz, 4H; *p*- $\text{C}_6\text{H}_4\text{Cl}$), 7.84 (d, $^3J(\text{H,H})$ = 8.32 Hz, 4H; *p*- $\text{C}_6\text{H}_4\text{Cl}$), 7.79–7.27 (m, 60H; PPh_3); $^{31}\text{P}\{^1\text{H}\}$ NMR (109.4 MHz, CDCl_3): δ = 21.6 (s; PPh_3); FAB-MS: m/z : 1022 [$M^+ - \text{PdCl}$], 760 [$M^+ - (\text{PPh}_3)\text{PdCl}$], 725 [$M^+ - (\text{PPh}_3)\text{PdCl}_2$], 667 [$(\text{Ph}_3\text{P})_2\text{PdCl}$]; UV/Vis (CHCl_3): λ_{max} (ϵ_{rel}) = 560 (1.0), 532 nm (0.85); elemental analysis calcd (%) for $\text{C}_{54}\text{H}_{38}\text{Cl}_4\text{N}_2\text{O}_2\text{P}_2\text{Pd}_2$ (1163.5): C 55.75, H 3.29, N 2.41; found: C 55.56, H 3.74, N 2.48.

Complexes 10a,c: [$L_n\text{MX}$] = $(\text{Ph}_3\text{P})_2\text{PtCl}_2$ (236 mg). The solvent was removed under reduced pressure at 60 °C, and the residue dissolved in CH_2Cl_2 (15 mL) and filtered (P3). The solutions were layered with *n*-

Table 4. Crystal structure data of compounds **4c**, **5a**, **6b**, **6c**, **6e**, **7c**, and **8c**.

	4c	5a	6b	6c	6e	7c	8c
formula	$\text{C}_{96}\text{H}_{76}\text{Cl}_{14}\text{Cu}_2\text{N}_2\text{O}_6\text{P}_2$	$\text{C}_{93}\text{H}_{76}\text{Ag}_2\text{Cl}_6\text{N}_2\text{O}_4\text{P}_2$	$\text{C}_{86}\text{H}_{46}\text{Au}_2\text{Cl}_6\text{N}_2\text{O}_2\text{P}_2$	$\text{C}_{54}\text{H}_{40}\text{Au}_2\text{Cl}_6\text{N}_2\text{O}_2\text{P}_2$	$\text{C}_{54}\text{H}_{40}\text{Au}_2\text{Cl}_6\text{N}_4\text{O}_2\text{P}_2$	$\text{C}_{32}\text{H}_{42}\text{Au}_2\text{Cl}_6\text{N}_2\text{O}_2\text{P}_2$	$\text{C}_{60}\text{H}_{56}\text{Au}_4\text{Cl}_{16}\text{N}_8\text{O}_4$
M_w [g mol $^{-1}$]	2100.97	1805.96	1471.54	1512.37	1445.47	1155.284	2308.25
crystal size [mm]	$0.30 \times 0.10 \times 0.10$	$0.22 \times 0.12 \times 0.02$	$0.53 \times 0.53 \times 0.10$	$0.47 \times 0.40 \times 0.10$	$0.53 \times 0.40 \times 0.13$	$0.24 \times 0.17 \times 0.11$	$0.15 \times 0.10 \times 0.07$
crystal system	triclinic	triclinic	triclinic	triclinic	triclinic	triclinic	triclinic
space group	$P\bar{1}$	$P\bar{1}$	$P\bar{1}$	$P\bar{1}$	$P\bar{1}$	$P\bar{1}$	$P\bar{1}$
a [Å]	12.683(2)	12.3720(16)	9.668(2)	10.285(2)	8.3752(9)	7.7686(8)	10.7244(10)
b [Å]	13.247(3)	13.0780(15)	11.450(4)	11.8523(13)	12.038(3)	9.8311(11)	12.0469(11)
c [Å]	16.676(3)	14.543(2)	12.7018(15)	12.835(2)	13.432(2)	12.6018(15)	16.7829(15)
α [°]	112.67(2)	95.999(15)	85.026(15)	90.569(10)	103.307(14)	91.475(14)	76.801(11)
β [°]	106.301(19)	93.261(16)	85.428(13)	106.128(14)	91.696(10)	94.755(14)	75.115(10)
γ [°]	86.86(2)	118.109(13)	87.28(2)	113.774(13)	96.945(13)	93.304(13)	65.637(1)
V [Å 3]	2477.0(8)	2049.0(5)	1395.2(6)	1362.2(4)	1305.9(4)	957.09(18)	1890.4(3)
Z	1	1	1	1	1	1	1
ρ_{calcd} [g cm $^{-3}$]	1.4085(5)	1.4636(4)	1.751	1.844	1.838	2.0044(4)	2.0276(3)
diffractometer	STOE IPDS	STOE IPDS	Nonius CAD4	Nonius Mach3	Nonius Mach3	STOE IPDS	STOE IPDS
radiation	$\text{MoK}\alpha$ (0.71073 Å)	$\text{MoK}\alpha$ (0.71073 Å)	$\text{MoK}\alpha$ (0.71073 Å)	$\text{MoK}\alpha$ (0.71073 Å)	$\text{MoK}\alpha$ (0.71073 Å)	$\text{MoK}\alpha$ (0.71073 Å)	$\text{MoK}\alpha$ (0.71073 Å)
T [K]	200	200	293	293	293	200	200
μ [mm $^{-1}$]	0.924	0.803	5.640	5.874	6.025	8.190	8.351
$F(000)$	1070	920	714	730	698	554	1092
2θ range [°]	1.67–23.79	1.79–24.05	2.51–23.98	2.69–23.97	2.45–23.97	2.60–27.96	1.87–23.96
index ranges	$-14 \leq h \leq 14$, $-14 \leq k \leq 15$, $-18 \leq l \leq 18$	$-14 \leq h \leq 13$, $-14 \leq k \leq 14$, $-16 \leq l \leq 16$	$0 \leq h \leq 11$, $-13 \leq k \leq 13$, $-14 \leq l \leq 14$	$0 \leq h \leq 11$, $-13 \leq k \leq 12$, $-14 \leq l \leq 14$	$0 \leq h \leq 9$, $-13 \leq k \leq 13$, $-15 \leq l \leq 15$	$-10 \leq h \leq 8$, $-12 \leq k \leq 12$, $-16 \leq l \leq 14$	$-12 \leq h \leq 12$, $-13 \leq k \leq 13$, $-19 \leq l \leq 19$
total reflections	13688	11965	4654	4529	4409	8248	10844
independent reflections	7050	6032	4358	4259	4093	4230	5543
observed reflections	2572	3337	3858	3764	3862	3813	4034
$[I > 2\sigma(I)]$							
parameters refined	551	486	364	325	316	208	434
R_1	0.0523	0.0529	0.0382	0.0359	0.0295	0.0242	0.0252
wR_2	0.1110	0.1163	0.1004	0.0887	0.0780	0.0571	0.0515
GOOF	0.749	0.817	1.089	1.021	1.097	1.024	0.847
residuals [e Å $^{-3}$]	−0.339/0.509	−1.031/0.935	−1.581/1.747	−1.015/2.035	−1.575/1.037	−1.852/1.083	−0.804/1.115

hexane (15 mL) and stored at -20°C for some days. Compounds **10a,c** crystallized as small red needles.

Compound 10a: Yield 182 mg (68%), red needles, m.p. 271°C (decomp); IR (KBr): $\tilde{\nu} = 3053, 1665, 1626, 1593, 1589, 1485, 1437, 1362, 1347, 1332, 1316, 1291, 1189, 1160, 1125, 1097, 1074, 1061, 1028, 1000, 822, 793, 744, 731, 701, 692, 618, 548, 528, 520, 498, 462, 445, 423\text{ cm}^{-1}$; ^1H NMR (270 MHz, CDCl_3): $\delta = 8.77$ (m, 4H; DPP- C_6H_5), 7.53 (m, 4H; DPP- C_6H_5), 7.31–7.00 (m, 60H; PPh_3); $^{31}\text{P}\{^1\text{H}\}$ NMR (109.4 MHz, CDCl_3): $\delta = 14.3$ (d, $^2J(\text{P,P}) = 18\text{ Hz}$; Cl–Pt–P), 7.4 (d, $^2J(\text{P,P}) = 18\text{ Hz}$; N–Pt–P); FAB-MS: m/z : 1796 $[M^+]$, 1761 $[M^+ - \text{Cl}]$, 1042 $[M^+ - (\text{Ph}_3\text{P})_2\text{PtCl}]$, 755 $[(\text{Ph}_3\text{P})_2\text{PtCl}]$, 719 $[(\text{Ph}_3\text{P})_2\text{Pt}]$; UV/Vis (CHCl_3): $\lambda_{\text{max}} (\epsilon_{\text{rel}}) = 536$ (1.0), 509 nm (0.9); fluorescence (CHCl_3): $\lambda_{\text{max}} = 577\text{ nm}$; $\Phi = 16\%$; elemental analysis calcd (%) for $\text{C}_{90}\text{H}_{70}\text{Cl}_2\text{N}_2\text{O}_2\text{P}_4\text{Pt}_2 \cdot 1\text{CHCl}_3$ (1915.3): C 57.01, H 3.71, N 1.46; found: C 55.88, H 3.71, N 1.99.

Compound 10c: Yield 229 mg (74%), red needles, m.p. $>300^{\circ}\text{C}$; IR (KBr): $\tilde{\nu} = 3053, 1698, 1623, 1590, 1485, 1437, 1405, 1339, 1305, 1277, 1188, 1159, 1117, 1094, 1014, 999, 833, 743, 703, 693, 619, 548, 527, 498, 460, 444, 424\text{ cm}^{-1}$; ^1H NMR (270 MHz, CDCl_3): $\delta = 8.47$ (d, $^3J(\text{H,H}) = 8.61\text{ Hz}$, 4H; DPP–CCHCH), 7.53 (d, $^3J(\text{H,H}) = 8.61\text{ Hz}$, 4H; DPP–CCH), 7.31–7.00 (m, 60H, PPh_3); $^{31}\text{P}\{^1\text{H}\}$ NMR (109.4 MHz, CDCl_3): $\delta = 13.8$ (d, $^2J(\text{P,P}) = 18\text{ Hz}$; Cl–Pt–P), 7.8 (d, $^2J(\text{P,P}) = 18\text{ Hz}$; N–Pt–P); FAB-MS: m/z : 1866 $[M^+]$, 754 $[(\text{Ph}_3\text{P})_2\text{PtCl}]$, 719 $[(\text{Ph}_3\text{P})_2\text{Pt}]$; UV/Vis (CHCl_3): $\lambda_{\text{max}} (\epsilon_{\text{rel}}) = 554$ (1.0), 572 nm (0.9); fluorescence (CHCl_3): $\lambda_{\text{max}} (I_{\text{rel}}) = 685$ (1.0), 625 nm (0.7); $\Phi = 13\%$; solid-state fluorescence: $\lambda_{\text{max}} = 635\text{ nm}$; elemental analysis calcd (%) for $\text{C}_{90}\text{H}_{68}\text{Cl}_3\text{N}_2\text{O}_2\text{P}_4\text{Pt}_2 \cdot 3\text{CHCl}_3$ (2213.9): C 50.20, H 3.19, N 1.26; found: C 49.06, H 3.57, N 1.66.

X-ray structure determination of compounds 4c, 5a, 6b, c, e, 7c, and 8c: Single crystals of these dye complexes were grown from saturated solutions in CHCl_3 or CH_2Cl_2 at 0°C (-20°C for **4c**) by covering them with a layer of *n*-hexane or diethyl ether, respectively. Crystal data collection parameters are summarized in Table 4. Intensity data were corrected for Lorentz and polarization effects, and absorption corrections were carried out. The structures were solved by direct methods (SHELXS-97 (**4c**),^[13] SIR-97 (**5a**, **7c**, **8c**),^[14] and SHELXS-86 (**6b,c,e**)^[15] and refined by the full-matrix least-squares method SHELX-97 (**4c**, **5a**, **7c**, **8c**)^[16] and SHELX-93 (**6b,c,e**).^[17] After applying anisotropic thermal parameters for non-hydrogen atoms, we calculated H-atom positions according to ideal geometry, and these were used only in structure factor calculations.^[18]

It should be mentioned that crystals of **4c** and **5a** contained small additional molecules, which could not be fully characterized. They were assigned as disordered formic acid and CH_2Cl_2 , respectively.

Acknowledgements

We thank the group of Prof. Dr. R. Gompper (†) for assistance in the field of dyes and the Fonds der Chemischen Industrie for financial support. The doctoral scholarship for M.L. of the Freistaat Bayern is appreciated.

- [1] H. Langhals, M. Limmert, I.-P. Lorenz, P. Mayer, H. Piotrowski, K. Polborn, *Eur. J. Inorg. Chem.* **2000**, 2345–2349.
- [2] A. Iqbal, M. Jost, R. Kirchmayr, J. Pfenninger, A. Rochat, O. Wallquist, *Bull. Soc. Chim. Belg.* **1988**, 97, 615–634.
- [3] H. Langhals, J. Karolin, L. B.-A. Johansson, *J. Chem. Soc. Faraday Trans.* **1998**, 94, 2919–2922.
- [4] T. Potrawa, H. Langhals, *Chem. Ber.* **1987**, 120, 1075–1078.
- [5] H. Langhals, T. Grundei, T. Potrawa, K. Polborn, *Liebigs Ann.* **1996**, 676–682.
- [6] H. Langhals, R. Ismael, O. Yürük, *Tetrahedron* **2000**, 56, 5435–5441.
- [7] J. A. McCleverty, M. M. M. da Mota, *J. Chem. Soc. Dalton Trans.* **1973**, 2571–2574.
- [8] D. Hock, K. Sünkel, W. Beck, *Z. Naturforsch. B: Chem. Sci.* **1999**, 54, 92–102, and references therein.
- [9] H. Langhals, *Nachr. Chem. Tech. Lab.* **1980**, 28, 716–718; [*Chem. Abstr.* **1981**, 95, R9816q].
- [10] M. Limmert, PhD thesis, LMU, Munich (Germany), **2001**.
- [11] C. A. McAuliffe, R. V. Parish, P. D. Randall, *J. Chem. Soc. Dalton Trans.* **1979**, 1730–1735.
- [12] G. Brauer, *Handbuch der Präparativen Anorganischen Chemie*, 3. Aufl., F. Enke Verlag, Stuttgart, **1981**, Bd. 3.
- [13] G. M. Sheldrick, *Acta Crystallogr. Sect. A* **1996**, 46, 467–473.
- [14] A. Altomare, M. C. Burla, M. Camalli, G. L. Cascarano, C. Giacovazzo, A. Guagliardi, A. G. G. Moliterni, G. Polidori, R. Spagna, *J. Appl. Crystallogr.* **1999**, 32, 115–119.
- [15] G. M. Sheldrick, SHELXS-86, Program for the Solution of X-ray Structures, University of Göttingen, Göttingen (Germany), **1986**.
- [16] G. M. Sheldrick, SHELXL-97, Program for Crystal Structure Refinement, University of Göttingen, Göttingen (Germany), **1997**.
- [17] G. M. Sheldrick, SHELXS-93, Program for Crystal Structure Refinement, University of Göttingen, Göttingen (Germany), **1993**.
- [18] CCDC-177250 (**4c**), CCDC-177252 (**5a**), CCDC-177116 (**6b**), CCDC-137742 (**6c**), CCDC-177117 (**6e**), CCDC-177249 (**7c**), and CCDC-177251 (**8c**) contain the supplementary crystallographic data for this paper. These data can be obtained free of charge via www.ccdc.cam.ac.uk/conts/retrieving.html (or from the Cambridge Crystallographic Data Centre, 12 Union Road, Cambridge CB2 1EZ, UK; fax: (+44) 1223-336-033; or e-mail: deposit@ccdc.cam.ac.uk).

Received: January 21, 2002 [F3812]